

# Experimental Demonstration of the Stabilization of Colloids by Addition of Salt

Sela Samin, Manuela Hod, Eitan Melamed, Moshe Gottlieb, and Yoav Tsori\*

*Department of Chemical Engineering and the Ilse Katz Institute for Nanoscale Science and Technology,  
Ben-Gurion University of the Negev, 84105 Beer-Sheva, Israel.*

\* To whom correspondence should be addressed; E-mail: [tsori@bgu.ac.il](mailto:tsori@bgu.ac.il)

(Dated: 28 August 2014)

We demonstrate a general non-Derjaguin-Landau-Verwey-Overbeek method to stabilize colloids in liquids. By this method, colloidal particles that initially form unstable suspension and sediment from the liquid are stabilized by the *addition* of salt to the suspending liquid. Yet, the salt is not expected to adsorb or directly interact with the surface of the colloids. For the method to work, the liquid should be a mixture, and the salt needs to be antagonistic such that each ion is preferentially solvated by a different component of the mixture. The stabilization may depend on the salt content, mixture composition, or distance from the mixture's coexistence line.

## I. INTRODUCTION

The stability of colloidal suspensions is important for the physical and chemical properties of pastes, paints and inks, and in a variety of other applications in material science. The van der Waals attraction between colloids can be overcome by steric repulsion, where surfactants or polymers are chemically or physically attached to the surface of the colloids and prevent them from aggregating [1]. In many cases these coatings are undesired because they change the surface chemistry, interfere with the activity of functional groups, block the contact between colloids once the suspension is dried, or affect the rheology of the liquid [2]. Alternatively, the colloidal dispersion may be stabilized electrostatically by means of charged molecules attached or adsorbed to the particle surface and the stability against aggregation is achieved by the Coulombic repulsion between the charged colloids. In the common Derjaguin-Landau-Verwey-Overbeek (DLVO) paradigm [3, 4], when salt is added to an electrostatically-stabilized colloidal dispersion, the range of repulsion, set by the Debye length  $\lambda_D$ , decreases and the colloids tend to aggregate [5, 6].

In recent years, the importance of the preferential solvation of ions in different solvents has been realized [7, 8] and used in emulsions of two immiscible liquids. Leunissen *et al.* [9–11] used the preferential solvation and resulting partitioning of antagonistic ion pairs to control the stability and organization of *charged* colloids. A recently published non-DLVO theory exploits ion solvation to predict that both neutral and charged colloids can be effectively suspended by the addition of salt [12] to homogeneous mixtures. The key requirements are that (i) the suspending medium is a mixture of liquids and (ii) the salt is antagonistic; namely, the cation and anion are preferentially solvated in the different solvents [13]. The ions are not required to interact with the surface of the colloidal particle. The main advantage of the proposed stabilization method over the prevailing practice is that the stabilization is mediated by the liquid itself without the presence of large molecules or the need to modify the particle's surface. The theory predicts that the underlying mechanism should be effective in aqueous mixtures and it has a unique dependence on temperature, salt content, and mixture composition. Here we demonstrate experimentally, with a select set of experiments on key combinations of particles and liquids, that indeed colloidal stabi-

lization can be achieved by the addition of antagonistic salts as predicted.

In order to test the theory [12], we study experimentally the behavior of two types of neutral colloids: micron-sized cross-linked polystyrene (PS) microspheres and graphene sheets exfoliated from graphite particles. Two types of liquid mixtures are employed: a mixture of water and 2,6-lutidine which has a lower critical solution temperature [14] and a mixture of water and acetonitrile which has an upper critical solution temperature (UCST) [15]. In the course of the experiments, we track the temporal behavior of the dispersions in each one of the two pure solution components alone, in the mixture in the presence of a nonantagonistic salt (NaCl), and in the presence of an antagonistic salt (NaBPh<sub>4</sub>). The suspensions of the PS microspheres are studied by dynamic light scattering (DLS), whereas for the graphite or graphene suspensions visible-light transmission spectroscopy is used. Cryo-TEM imaging is carried out to complement the information regarding the aggregation state, Zeta-potential measurements to ascertain particle neutrality, and contact-angle measurements to determine the affinity of the mixture components to the solid surface.

According to the theory, the suspending efficiency of the proposed mechanism depends on the solvent-mixture composition, salt concentration, and the temperature  $T$  in terms of its distance from the coexistence line temperature  $T_c$ . The sensitivity to the experimental variables is clearly demonstrated in Fig. 4 of Ref. [12]. Rather than carry out an extensive search for the proper conditions, we use the theory, adjusted to correspond to the experimental systems at hand, to provide the guidelines for the judicious choice of the experimental parameters. In what follows, we provide a brief account of the theory [12] with the required modifications and calculation pertaining to the experimental systems described above.

For colloids immersed in a generic mixture of two solvents, the total free energy is given as a sum of volume and surface contributions  $F = \int (f_m + f_{es} + f_{ion}) d\mathbf{r} + \int f_\gamma d\mathbf{r}_s$ , where  $\mathbf{r}_s$  is a vector on the surface.  $f_m$  is the mixing free energy density given by [16]

$$a^3 f_m = k_B T [\phi \log \phi + (1 - \phi) \log(1 - \phi) + \chi \phi(1 - \phi)] + \frac{1}{2} C (\nabla \phi)^2. \quad (1)$$

Here  $\phi$  is the *local* mole fraction of the more polar solvent,

$k_B$  is the Boltzmann constant,  $T$  is the temperature,  $\chi \sim 1/T$  is the Flory-Huggins interaction parameter,  $a$  is a molecular length, and  $C$  is a constant. The short-range interfacial interaction of the mixture with the solid colloid surface is given by  $f_\gamma = \Delta\gamma\phi(\mathbf{r}_s) + \sigma\psi(\mathbf{r}_s)$ , where  $\Delta\gamma$  is the difference between the surface tensions of the two liquids and the solid (assumed chemically homogeneous) and  $\sigma$  is the surface charge density of the colloid. A positive  $\Delta\gamma$  means the surface prefers the less polar cosolvent. The new stabilization mechanism is not based on specific interactions between the ions and the surface [17, 18], and hence these are not included here. The electrostatic energy density  $f_{\text{es}} = -(1/2)\varepsilon(\phi)(\nabla\psi)^2$  is expressed by the local electrostatic potential  $\psi$  and the constitutive relation between the dielectric constant and mixture composition  $\varepsilon(\phi)$ , assumed linear.

The Gibbs transfer energy of moving an ion from one solvent to another gives rise to numerous important interfacial phenomena [19–21] and can even lead to flocculation of colloids [22]. In the present context and for a monovalent salt, the ions' entropy, electrostatic energy, and preferential solvation is modeled by

$$f_{\text{ion}} = k_B T \{ n^+ [\log(a^3 n^+) - 1] + n^- [\log(a^3 n^-) - 1] \} + e(n^+ - n^-)\psi - k_B T (\Delta u^+ n^+ + \Delta u^- n^-) \phi. \quad (2)$$

Here  $n^\pm$  are the average ion number density in the system, and  $e$  is the elementary charge. The parameters  $\Delta u^\pm$  express the affinity of the positive and negative ions toward the polar phase [10, 18, 23, 24]. When the antagonistic salt used here,  $\text{NaBPh}_4$ , is added to the mixture of water and 2,6-lutidine the  $\text{Na}^+$  cation is hydrophilic with  $\Delta u^+ \simeq 6$ , while the  $\text{BPh}_4^-$  anion is hydrophobic with  $\Delta u^- \simeq -16$  [25, 26], and thus both requirements (i) and (ii) listed above hold. The colloids will be stabilized irrespective of the sign of  $\Delta\gamma$  or  $\Delta u^\pm$  and as long as  $|\Delta u^+ - \Delta u^-|$  is large enough.

In equilibrium the composition  $\phi$ , ion densities  $n^\pm$ , and electrostatic potential  $\psi$  satisfy the three coupled equations  $\delta F/\delta\phi = 0$ ,  $\delta F/\delta n^\pm = 0$ , and the Poisson equation  $\delta F/\delta\psi = 0$ . The boundary conditions at the colloid surface are  $\mathbf{n} \cdot \nabla\psi = \sigma/\varepsilon(\phi)$  and  $\mathbf{n} \cdot \nabla\phi = -\Delta\gamma/C$ , where  $\mathbf{n}$  is a unit vector normal to the colloid surface. We calculate the interaction between two neutral spherical colloids of radius  $R$  separated by a distance  $D$  and immersed in a mixture at average composition  $\phi_0$  and ion density  $n_0$  as follows. We begin by solving the governing equations for two flat plates a distance  $D$  apart. Once the equilibrium profiles are known the pressure tensor  $P_{ik} = (\phi\delta f/\delta\phi + n^+\delta f/\delta n^+ + n^-\delta f/\delta n^- - f)\delta_{ik} - \varepsilon E_i E_k$  is obtained [27, 28]. Here  $\mathbf{E} = -\nabla\psi$  is the electric field. We define  $\Omega$  as the integral of the osmotic pressure from  $D$  to  $\infty$ . When the distance between the colloids is much smaller than their size,  $D \ll R$ , Derjaguin's approximation holds and the total effective colloid potential is [2]

$$U(D) = \pi R \int_D^\infty \Omega(D') dD' - \frac{AR}{12D}, \quad (3)$$

where  $A$  is Hamaker's constant. In Eq. 3, we use a simple form of van der Waals interaction, not taking into account

the wetting close to the colloid [29] and screening by the salt [30]. The wetting layer around a hydrophobic colloid in the water–2,6-lutidine mixture increases the van der Waals attraction [29], though in our experiments the effect is expected to be small, since the temperature is kept relatively far from  $T_c$ . In addition, as will be demonstrated below, we do not observe stable suspension when the hydrophilic salt ( $\text{NaCl}$ ) is added, and this result implies that salt screening of van der Waals interaction alone is not enough to stabilize the colloids. We stress that the aim of the simple theory we use is to isolate one possible mechanism and show that it can be comparable to or even larger than others in the stabilization.

Insight can be gained by a standard linear theory valid when  $e\psi \ll k_B T$  and  $|\Delta u^\pm(\phi - \phi_0)| \ll 1$  hold. The potential and composition are then given as a sum of four exponentials  $e^{\pm q_i z}$  with the two wave numbers  $q_i$  ( $i = 1, 2$ ) given by  $q_1^2 q_2^2 = 1/(\xi\lambda_D)^2$  and  $q_1^2 + q_2^2 = 1/\lambda_D^2 - 1/\xi^2 - 2n_0(\Delta u^+ - \Delta u^-)^2/C$ , where  $\xi$  is the correlation length modified by the salt [18, 21, 31]. For electrically neutral colloids ( $\sigma = 0$ ), the amplitudes of the exponentials are proportional to the difference in wettability of the two solvents,  $\Delta\gamma$ , and the height of the barrier  $U(D_{\text{max}})$  is proportional to  $(\Delta\gamma)^2$ . When a value of approximately 10 mM of salt is used in the analytical expressions, it follows that the barrier location  $D_{\text{max}}$  is in the range 5–15 nm and the barrier height can be significantly larger than approximately  $3k_B T$  thus preventing colloidal coagulation.

## II. EXPERIMENTAL DETAILS

### A. Preparation and characterization of polymer colloids

The spherical colloidal particles are synthesized by using distillation-precipitation polymerization of divinylbenzene [32]. The size distribution and shape are determined by means of scanning electron microscopy using JSM-7400F (JEOL) ultrahigh-resolution cold field-emission gun SEM; see Fig. S2 in the Supplemental Material [33].

For the surface charge measurement, the colloids are dispersed in ethanol, and their  $\zeta$  potential is measured on a Zetasizer Nano ZS (Malvern) at 298 K using a universal dip cell. The measured peak value of the  $\zeta$  potential is  $0 \pm 2$  mV.

### B. DLS of polymer particles

The mixture of water (deionized to a resistivity of 18.2 M $\Omega$  cm) and 2,6-lutidine (Sigma-Adrich, purified by redistillation,  $\geq 99\%$ ) with 71 wt% water is prepared at ambient temperature. The addition of the polymer microspheres to the samples for the DLS experiments is performed in two steps. First, the colloids are weighed and 1 ml of the water–2,6-lutidine mixture and salt are added. The sample containing the particles is then placed in the ultrasonic bath and sonicated for 15 min. After sonication, it is diluted with the same water-

lutidine mixture, shaken, and further sonicated for 3 – 5 min. Subsequently, it is equilibrated at the required temperature ( $T = T_t - 6$  K) by waiting for 10 min.

DLS is measured on the CGS-3 equipped with a LSE-5004 cross-correlator (ALV, Germany) at a constant angle of  $90^\circ$  using clear glass vials (Sigma-Aldrich). Phase diagrams are separately determined for the mixture in the absence of salt and after the addition of 20 mM NaBPh<sub>4</sub> (see Fig. S5 in the Supplemental Material [33]). For the solution mixture in the absence of salt at a water weight fraction of 0.71 ( $\phi=0.935$ ),  $T_t = 307$  K, and experiments are carried out at  $T = 301$  K. With the salt  $T_t = 321$  K, and experiments are carried out at  $T = 315$  K. During the experiment, the temperature is kept constant to within 0.1 K by using a Julabo CF31 thermostat. Each measurement consists of five runs of 10e each and is carried out at a beam wavelength of 632.8 nm. The CONTIN algorithm is used for the extraction of the data. The Stokes-Einstein relation is employed for the calculation of the hydrodynamic radius  $R_h$ . Since temperature and salt impact the viscosity, we determine the viscosity for each sample by using a Cannon-Fenske viscometer at the appropriate temperature and composition: (i) no salt mixture –  $T = 301$  K,  $\eta=2.25$  mPa s; (ii) mixture with 20 mM NaBPh<sub>4</sub> –  $T = 315$  K,  $\eta=1.98$  mPa s; (iii) mixture at  $T = 305$  K, 20 mM antagonistic salt –  $\eta=2.12$  mPa s; 25 mM salt –  $\eta=2.16$  mPa s. The mass-weighted DLS data are smoothed using cubic interpolation. The synthesis yields also smaller particles with diameter  $< 500$  nm. The contribution of these small colloids to the total measured intensity is negligible and therefore not shown.

### C. Preparation of graphene

Graphite flakes are purchased from Sigma-Aldrich and used as received. For each experiment 0.1 wt% are mixed with the respective mixture and placed in a sonicator bath (Elma, S 10 Elmasonic, Germany) for 3 h to allow exfoliation. The sonicator is operated under ice-cooling in order to prevent heating and keep the temperature at approximately 273 K throughout the process. To separate the resulting graphene sheets from nonexfoliated graphite flakes, samples are centrifuged at a constant temperature (Hermle Z383K, R-max 9.6 cm, Germany, 277 K) at a rate of 1000 rpm for 5 min.

### D. Visible-light transmission in graphene dispersions

The visible-light transmission through the graphene dispersions is measured by a Jasco V-530 UV-visible spectrometer at a wavelength of 660 nm. We measure the transmission in different mixtures of water (deionized to a resistivity of 18.2 M $\Omega$  cm) and acetonitrile (Sigma-Aldrich, anhydrous 99.8%). Transmission values are converted into graphene concentration by using an extinction coefficient of  $3.0 \times 10^3$  l g<sup>-1</sup> m<sup>-1</sup> taken from the literature [34]. The error in the concentration

is estimated from the standard deviation of several measurements for a mixture with 20 wt% acetonitrile and the antagonistic salt.

## III. RESULTS

Because of the coupling between the mixture composition, salt concentration, and temperature (distance from coexistence line  $|T - T_t|$ ) we carry out a somewhat crude iterative process. The full nonlinear potential is calculated repeatedly for different salt concentrations and temperatures. Eventually, we settle on a set of values which, conceded, are not optimized but provide the essence of the stabilization mechanism. Figure 1 shows the full nonlinear potential  $U(D)$  vs temperature and salt content. The solid surface has a short-range chemical attraction to one of the solvents. For a hydrophobic colloid, water is depleted from its surface, and due to the preferential solvation of the ions, the vicinity of the surface has more hydrophobic than hydrophilic ions [see Figure S1 (a) in the Supplemental Material [33]]. In the case of a hydrophilic colloid, the more hydrophilic ions are enriched near it. Thus, the colloid becomes effectively charged when *either* of the solvents is adsorbed at the surface and entropically driven repulsion appears at large distances [9–11]. The potential has a barrier at  $D = D_{\max}$  and is attractive when  $D < D_{\max}$  due to van der Waals attraction and critical adsorption [35]. As salt is added,  $D_{\max}$  shifts to lower values while the potential barrier increases. Guided by the results of the calculation we opt to use a salt concentration of  $n_0 \approx 20$  mM and  $|T - T_t| \approx 6$  K. At this point, to further refine the correspondence between theory and experiment, the phase diagram for water–2,6-lutidine with 20 mM of NaBPh<sub>4</sub> is obtained ( $\phi_c = 0.879$  and  $T_c = 311$  K; see Fig. S5 in the Supplemental Material [33]). Relying on the phase diagram and the fact that the colloids are hydrophobic, we select for the experiments a solvent mixture with a water weight fraction of 0.71 ( $\phi_0 = 0.935$ ), for which  $T_t = 321$  K and hence  $|T_c - T_t| = 10$  K as in Fig. 1. The calculated salt-concentration dependence at the selected temperature and mixture composition is shown in Fig. 1(b), pointing towards the choice of 20 mM salt concentration.

### A. Experimental validation I

Cross-linked polystyrene colloids are prepared by using distillation-precipitation polymerization. Their radius is determined by scanning electron microscopy to be  $R = 0.85 \pm 0.3$   $\mu$ m, and their  $\zeta$  potential is found to be zero. The colloids and antagonistic (NaBPh<sub>4</sub>) or nonantagonistic (NaCl) salts are added to the mixture of water–2,6-lutidine.

Visual inspection shows that the colloids coagulate and sediment in pure lutidine, in the mixture without salt, or when the salt is not antagonistic (NaCl). However, when the antagonistic salt is added, the colloids remain suspended over a long time. When the antagonistic salt is added to pure lutidine, the colloids coagulate immediately. This result supports the notion that there is no significant direct chemical interaction

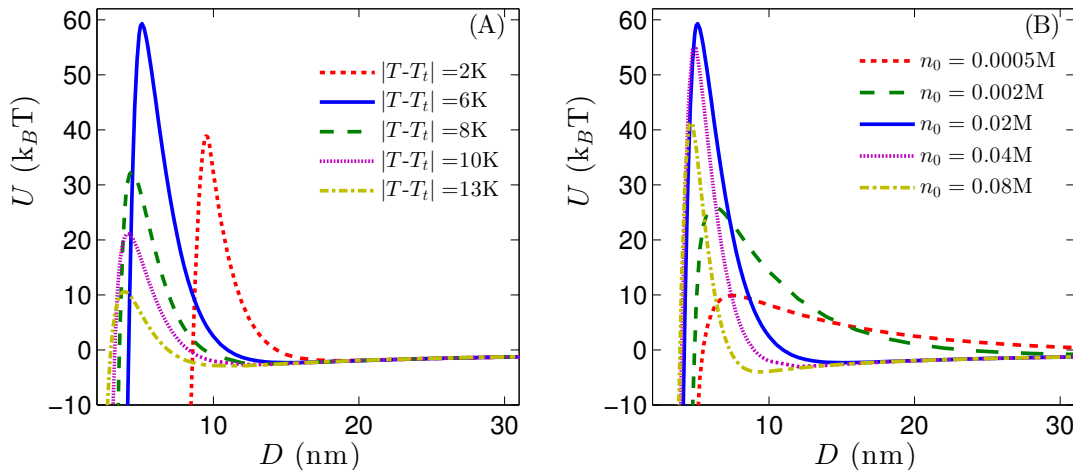


FIG. 1. Calculated effective potential between two colloids  $U(D)$  from Eq. (3) vs colloid surface separation  $D$  for varying temperatures  $T$  (a) and salt concentrations  $n_0$  (b). The location of the barrier peak at  $D_{\max}$  decreases with increasing distance from the coexistence line  $|T - T_t|$  or with increasing salt  $n_0$  ( $\lambda_D$  decreases). The mixture composition is such that  $|T_c - T_t| = 10$  K. In (a)  $n_0 = 20$  mM is constant while in (b)  $|T - T_t| = 6$  K is constant. For the water-2,6-lutidine mixture containing the antagonistic salt NaBPh<sub>4</sub> we used  $T_c = 311$  K,  $a = 3.4$  Å,  $C = \chi/a$ ,  $\varepsilon_{2,6\text{-lutidine}} = 6.9$ ,  $\varepsilon_{\text{water}} = 79.5$ ,  $\Delta\gamma = 0.1k_B T a^{-2}$ , and  $\Delta u^+ = -\Delta u^- = 8$ . For the colloidal PS particles we used  $R = 1$   $\mu\text{m}$  and  $A = 2 \times 10^{-21}$  J.

of the ions with the colloids. These qualitative observations are quantified by DLS for samples at  $|T - T_t| = 6$  K. Fig. 2(a) shows that the distribution of sizes shifts in time to larger aggregates when no salt is added to the mixture. The distributions in Fig. 2(b), corresponding to an addition of 20 mM NaCl, are similar in nature, and the size of aggregates shifts to larger values with increasing time until they sediment. This behavior is commonplace for neutral or slightly charged particles, and it is revealed in our numerical calculation [12] assuming hydrophilic salt ( $\Delta u^+ = \Delta u^-$ ) even if the colloids' surface potential is as large as 30 mV. A very different behavior is observed for the antagonistic salt, as shown in Fig. 2(c) and Fig. 2(d), where the aggregates are small and stable throughout the entire measurement period of 20 min.

Based on the theoretical calculations shown in Fig. 1(a) the energy barrier for aggregation at  $|T - T_t| > 13$  K should be very low, favoring aggregation. This result is confirmed by examining a 20-mM and 25-mM solutions of the antagonistic salt at  $T = 305$  K ( $|T - T_t| = 16$  K) as clearly indicated by the increase in size of the aggregates depicted in Fig. 3.

## B. Experimental validation II

To demonstrate the wide scope of the dispersion principle, we test it with a different type (carbonaceous) and shape (sheets) of colloid and different solvent mixture (UCST type). Measurements are carried out at room temperature in a mixture of water and acetonitrile (UCST,  $T_c \simeq 272$  K at a water mole fraction  $\phi_c \simeq 0.64$ ). Carbon-based colloids, which disperse in pure 2,6-lutidine, do not disperse in pure water or in acetonitrile.

We use ultrasonication to exfoliate graphene from graphite

flakes. UV-visible spectrometry of the suspensions is performed by measuring the transmission intensity at a wavelength of 660 nm. The transmission values are converted to concentration estimates with the Beer-Lambert law by using a literature value for the extinction coefficient [34]. For a mixture (80 wt%,  $\phi = 0.90$ ) with 20 mM NaCl or in the absence of salt, the transmission after  $t = 0.5$  h is 100% within the experimental error and therefore no dispersion of graphene is obtained. The same holds for pure acetonitrile and water. However, as shown in Fig. 4, the addition of an antagonistic salt results in the exfoliation of graphite, and a dispersion of graphene is obtained at mixture compositions  $\phi \gtrsim \phi_c$  (see also Fig. S4 in the Supplemental Material [33]). A small amount of graphene ( $\approx 0.03$  g l<sup>-1</sup>) is dispersed even in pure water with NaBPh<sub>4</sub>. We speculate that this dispersion is due to a specific interaction of the hydrophobic BPh<sub>4</sub><sup>-</sup> ions and the graphite, which can be incorporated into the theory [18]. The dispersion is enhanced more than twofold when the antagonistic salt is added to mixtures in the composition range  $0.85 \lesssim \phi \lesssim 0.95$ . This increase cannot be accounted for by an ion-surface interaction, since BPh<sub>4</sub><sup>-</sup> ions are expected to adsorb less in the mixture containing a nonpolar component. No stabilization is observed when the antagonistic salt is added to pure acetonitrile. The optimal dispersion at off-critical and water-rich mixtures is in agreement with the theoretical prediction in Fig. 4 of Ref. [12] for a hydrophobic surface. The concentration of graphene decays slowly to about 25% of its value at  $t = 0.5$  h within 24 h. However, for the sample with  $\phi = 0.901$ , many graphene sheets are clearly observed in cryo-TEM images taken 3 months after the sample preparation (see Fig. S4 in the Supplemental Material [33]), indicating a stable dispersion.

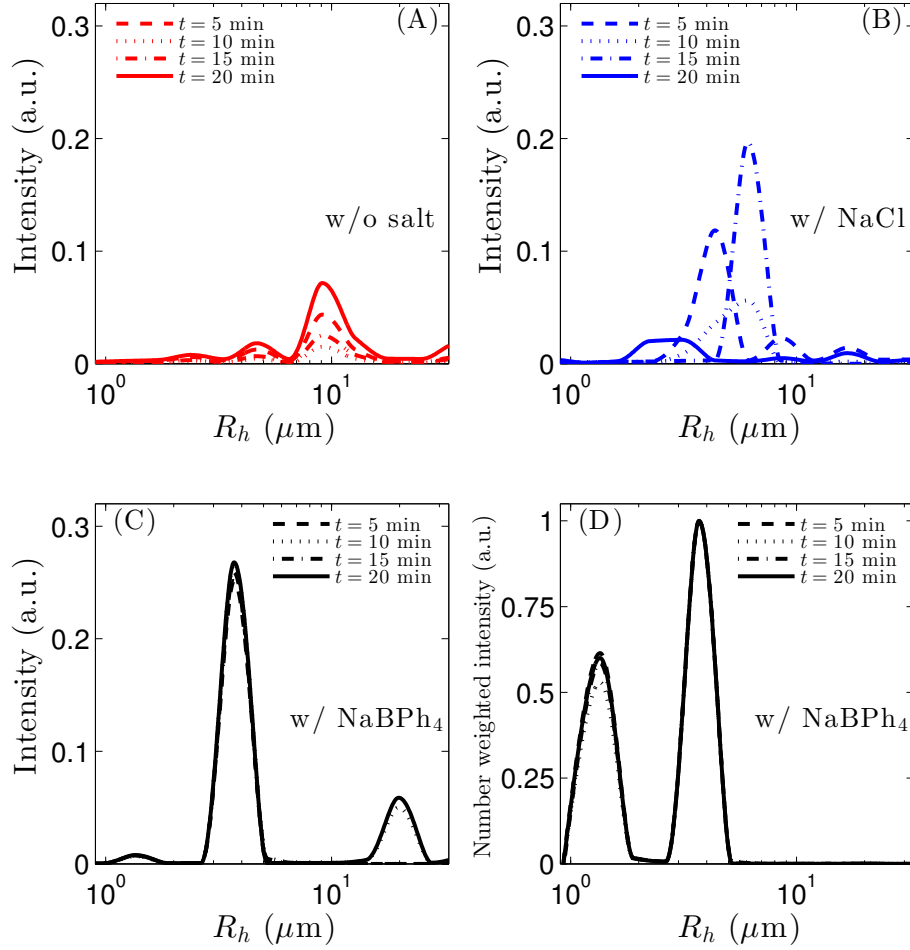


FIG. 2. (a)-(c) Colloidal mass-weighted distribution vs hydrodynamic radius  $R_h$ , as obtained by dynamic light scattering. Curves show distributions of polystyrene colloids in mixtures of water and 2,6-lutidine at different times (a) when no salt is added, (b) with 20 mM of NaCl, and (c) with 20 mM of the antagonistic salt NaBPh<sub>4</sub>. Without salt or with NaCl, colloids form aggregates that grow in time and eventually sediment from the solution. With the antagonistic salt, the aggregates are small and stable for the duration of the experiment. (d) Number-weighted distributions for the suspension with NaBPh<sub>4</sub>. All measurements are at  $|T - T_t| = 6$  K.

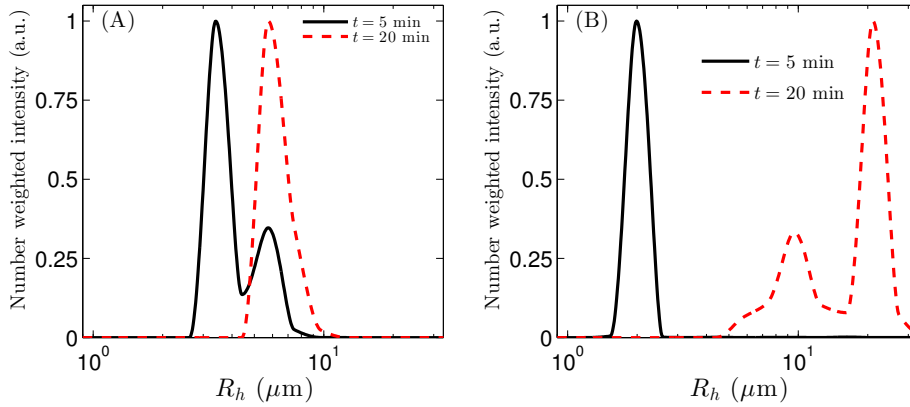


FIG. 3. Colloidal number-weighted distribution vs hydrodynamic radius  $R_h$ , as obtained by DLS. Curves show distributions of polystyrene colloids in mixtures of water and 2,6-lutidine at  $T = 305$  K. (a) With 20 mM of the antagonistic salt NaBPh<sub>4</sub>,  $|T - T_t| = 16$  K, and (b) with 25 mM of the antagonistic salt. In both cases, colloids form aggregates that grow in time and eventually sediment from the solution.

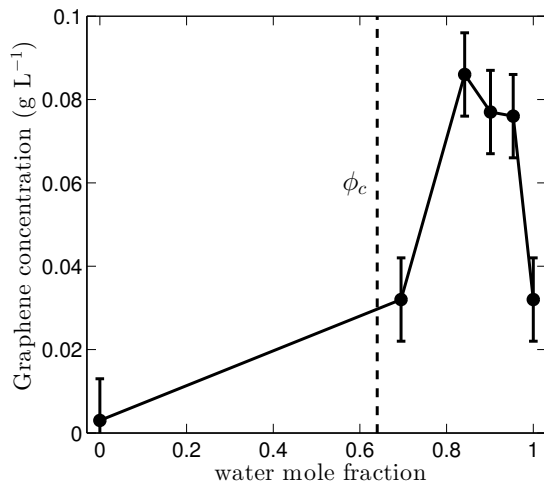


FIG. 4. Concentration of graphene dispersed in mixtures of water and acetonitrile containing 20 mM of NaBPh<sub>4</sub> at  $t = 0.5$  h. UV-visible transmission measurements are performed at room temperature  $|T - T_i| > 25$  K. The dashed line is the critical water mole fraction. As clearly observed at concentrations above critical,  $0.85 \lesssim \phi \lesssim 0.95$ , exfoliated graphene sheets remain dispersed in the liquid mixture. Dispersed graphene sheets are found even after 3 months.

### C. Experimental validation III

When NaBPh<sub>4</sub> is added to the mixture of water, acetonitrile, and cross-linked-polymer microspheres, the concentration of dispersed polymer colloids is increased by a mere

20%–30%. The reason for this relatively modest increase compared to the one observed in a mixture of water and 2,6-lutidine can be traced to the fact that acetonitrile is significantly less hydrophobic than lutidine, and hence the value of  $\Delta\gamma$  is too small for an effective stabilization; see Fig. S3 in the Supplemental Material [33].

Dispersion of colloids by the addition of salts is a versatile method and straightforward in practice. It has a unique dependence on temperature and composition and does not rely on direct adsorption of the ions on the colloids. We do not attempt to optimize the preparation protocol (e.g., longer or repeated tip sonication, different salt concentrations or variations in temperature or in mixture composition). Such an optimization is expected to greatly enhance the dispersion efficiency, and thus the method outlined above could be potentially useful in many cases where surfactants or grafting with polymers is inadequate. For example, graphene is conventionally dispersed with surfactants and is subsequently spin-coated on a substrate. Currently, the coating is transparent, but the surfactants degrade the in-plane conductivity; we speculate that replacing the surfactants with salt that is not adsorbed to the particle’s surface will increase this conductivity significantly.

### ACKNOWLEDGMENTS

Y. T. acknowledges support from the European Research Council “Starting Grant” No. 259205, COST Action MP1106, and Israel Science Foundation Grants No. 11/10 and No. 56/14.

S.S. and M. H. contributed equally to this work.

- 
- [1] Philip Pincus, “Colloid stabilization with grafted polyelectrolytes,” *Macromolecules* **24**, 2912 (1991).
  - [2] W. B. Russel, D. A. Saville, and W. R. Showalter, *Colloidal Dispersions* (Cambridge University Press, Cambridge, England, 1989).
  - [3] B. V. Derjaguin and L. D. Landau, “Theory of the stability of strongly charged lyophobic sols and the adhesion of strongly charged particles in solutions of electrolytes,” *Acta Physicochim URSS* **14**, 633 (1941).
  - [4] E. J. W. Verwey and J. Th. G. Overbeek, *Theory of the Stability of Lyophobic Colloids* (Elsevier, Amsterdam, 1948).
  - [5] Anand Yethiraj and Alfons van Blaaderen, “A colloidal model system with an interaction tunable from hard sphere to soft and dipolar,” *Nature (London)* **421**, 513 (2003).
  - [6] Mirjam E. Leunissen, Christina G. Christova, Antti-Pekka Hynninen, C. Patrick Royall, Andrew I. Campbell, Arnout Imhof, Marjolein Dijkstra, René van Roij, and Alfons van Blaaderen, “Ionic colloidal crystals of oppositely charged particles,” *Nature (London)* **437**, 235 (2005).
  - [7] Koichiro Sadakane, Akira Onuki, Koji Nishida, Satoshi Koizumi, and Hideki Seto, “Multilamellar structures induced by hydrophilic and hydrophobic ions added to a binary mixture of d<sub>2</sub>O and 3-methylpyridine,” *Phys. Rev. Lett.* **103**, 167803 (2009).
  - [8] Koichiro Sadakane, Michihiro Nagao, Hitoshi Endo, and Hideki Seto, “Membrane formation by preferential solvation of ions in mixture of water, 3-methylpyridine, and sodium tetraphenylborate,” *J. Chem. Phys.* **139**, 234905 (2013).
  - [9] Mirjam E. Leunissen, Alfons van Blaaderen, Andrew D. Hollingsworth, Matthew T. Sullivan, and Paul M. Chaikin, “Electrostatics at the oil-water interface, stability, and order in emulsions and colloids,” *Proc. Natl. Acad. Sci. U.S.A.* **104**, 2585 (2007).
  - [10] Mirjam E. Leunissen, Jos Zwanikken, René van Roij, Paul M. Chaikin, and Alfons van Blaaderen, “Ion partitioning at the oil-water interface as a source of tunable electrostatic effects in emulsions with colloids,” *Phys. Chem. Chem. Phys.* **9**, 6405 (2007).
  - [11] Jos Zwanikken and René van Roij, “Charged colloidal particles and small mobile ions near the oil-water interface: Destruction of colloidal double layer and ionic charge separation,” *Phys. Rev. Lett.* **99**, 178301 (2007).
  - [12] Sela Samin and Yoav Tsoi, “Stabilization of charged and neutral colloids in salty mixtures,” *J. Chem. Phys.* **139**, 244905 (2013).
  - [13] Yizhak Marcus, *Ion Solvation* (Wiley, New York, 1985).
  - [14] Carlos A. Grattoni, Richard A. Dawe, C. Yen Seah, and Jane D. Gray, “Lower critical solution coexistence curve and physical properties (density, viscosity, surface tension, and interfacial tension) of 2,6-lutidine + water,” *J. Chem. Eng. Data* **38**, 516

- (1993).
- [15] J. A. Renard and A. G. Oberg, "Ternary systems: Water-acetonitrile-salts." *J. Chem. Eng. Data* **10**, 152 (1965).
- [16] Samuel Safran, *Statistical Thermodynamics of Surfaces, Interfaces, and Membranes* (Westview Press, New York, 1994).
- [17] Robert J. Hunter, *Foundations of Colloid Science*, 2nd ed. (Oxford University, New York, 2001).
- [18] Ryuichi Okamoto and Akira Onuki, "Charged colloids in an aqueous mixture with a salt," *Phys. Rev. E* **84**, 051401 (2011).
- [19] Yan Levin, "Polarizable ions at interfaces," *Phys. Rev. Lett.* **102**, 147803 (2009).
- [20] Yan Levin, Alexandre P. dos Santos, and Alexandre Diehl, "Ions at the air-water interface: An end to a hundred-year-old mystery?" *Phys. Rev. Lett.* **103**, 257802 (2009).
- [21] Ursula Nellen, Julian Dietrich, Laurent Helden, Shirish Chodankar, Kim Nygård, J. Friso van der Veen, and Clemens Bechinger, "Salt-induced changes of colloidal interactions in critical mixtures," *Soft Matter* **7**, 5360 (2011).
- [22] Roland R. Netz, "Colloidal flocculation in near-critical binary mixtures," *Phys. Rev. Lett.* **76**, 3646–3649 (1996).
- [23] S. Samin and Y. Tsori, "Attraction between like-charge surfaces in polar mixtures," *Europhys. Lett.* **95**, 36002 (2011).
- [24] M. Bier, A. Gambassi, M. Oettel, and S. Dietrich, "Electrostatic interactions in critical solvents," *EPL* **95**, 60001 (2011).
- [25] Halina D. Inerowicz, Wei Li, and Ingmar Persson, "Determination of the transfer thermodynamic functions for some monovalent ions from water to *N,N*-dimethylthioformamide, and for some anions from water to methanol, dimethyl sulfoxide, acetonitrile and pyridine, and standard electrode potentials of some M+/M(s) couples in *N,N*-dimethylthioformamide," *J. Chem. Soc. Faraday Trans.* **90**, 2223 (1994).
- [26] 2,6-lutidine is a structural analog of pyridine. Hence, Gibbs transfer energies are estimated from the data for a water-pyridine mixture in Ref. [25].
- [27] L. D. Landau, E. M Lifshitz, and L. P. Pitaevskii, *Electrodynamics of Continuous Media*, 2nd ed. (Butterworth-Heinemann, Amsterdam, 1984).
- [28] Dan Ben-Yaakov, David, Andelman Daniel Harries, and Rudi Podgornik, "Ions in mixed dielectric solvents: Density profiles and osmotic pressure between charged interfaces," *J. Phys. Chem. B* **113**, 6001 (2009).
- [29] B. M. Law, J.-M. Petit, and D. Beysens, "Adsorption-induced reversible colloidal aggregation," *Phys. Rev. E* **57**, 5782 (1998).
- [30] V. A. Parsegian, *Van der Waals Forces: A Handbook for Biologists, Chemists, Engineers, and Physicists* (Cambridge University Press, Cambridge, England, 2005).
- [31] Markus Bier, Andrea Gambassi, and Siegfried Dietrich, "Local theory for ions in binary liquid mixtures," *J. Chem. Phys.* **137**, 034504 (2012).
- [32] Feng Bai, Bo Huang, Xinlin Yang, and Wenqiang Huang, "Synthesis of monodisperse porous poly(divinylbenzene) microspheres by distillation-precipitation polymerization," *Polymer* **48**, 3641 (2007).
- [33] "See supplemental material at <http://link.aps.org/supplemental/10.1103/physrevapplied.2.024008> for information regarding experimental details and procedures and numerical calculations."
- [34] Matat Buzaglo, Michael Shtein, Sivan Kober, Robert Lovrincic, Ayelet Vilan, and Oren Regev, "Critical parameters in exfoliating graphite into graphene," *Phys. Chem. Chem. Phys.* **15**, 4428 (2013).
- [35] R. Evans, U. Marini Bettolo Marconi, and P. Tarazona, "Fluids in narrow pores: Adsorption, capillary condensation, and critical points," *J. Chem. Phys.* **84**, 2376 (1986).